

Time-series expression profiles of mRNAs and lncRNAs during mammalian palatogenesis

Wenbin Huang^{1,2} | Wenjie Zhong^{2,3,4} | Qing He⁵ | Yizhu Xu^{6,7} | Jiuxiang Lin^{1,2} |
Yi Ding⁵ | Huaxiang Zhao^{6,7}  | Xiaowen Zheng^{8,9,10} | Yunfei Zheng^{1,2} 

¹Department of Orthodontics, Peking University School and Hospital of Stomatology, Beijing, China

²National Center of Stomatology, National Clinical Research Center for Oral Diseases, National Engineering Laboratory for Digital and Material Technology of Stomatology, Beijing Key Laboratory of Digital Stomatology, Research Center of Engineering and 3-Technology for Computerized Dentistry Ministry of Health, NMPA Key Laboratory for Dental Materials, Peking University School and Hospital of Stomatology, Beijing, China

³The Affiliated Stomatology Hospital, Chongqing Medical University, Chongqing, China

⁴Chongqing Key Laboratory of Oral Diseases and Biomedical Sciences, Chongqing, China

⁵Department of Physiology and Pathophysiology, School of Basic Medical Sciences, Xi'an Jiaotong University Health Science Center, Xi'an, China

⁶Key Laboratory of Shaanxi Province for Craniofacial Precision Medicine Research, College of Stomatology, Xi'an Jiaotong University, Xi'an, China

⁷Department of Orthodontics, College of Stomatology, Xi'an Jiaotong University, Xi'an, China

⁸Department of Orthodontics, Shanghai Ninth People's Hospital, College of Stomatology, Shanghai Jiao Tong University School of Medicine, Shanghai, China

⁹National Clinical Research Center for Oral Disease, Shanghai, China

¹⁰Shanghai Key Laboratory of Stomatology &, Shanghai Research Institute of Stomatology, Shanghai, China

Correspondence

Huaxiang Zhao, Key Laboratory of Shaanxi Province for Craniofacial Precision Medicine Research, College of Stomatology, Xi'an Jiaotong University, 710004 Xi'an, Shaanxi, China.
Email: huaxiangzhao@xjtu.edu.cn

Xiaowen Zheng, Department of Orthodontics, Shanghai Ninth People's Hospital, College of Stomatology, Shanghai Jiao Tong University School of Medicine, 200011 Shanghai, China.
Email: xiaowenzheng1027@qq.com

Yunfei Zheng, Department of Orthodontics, Peking University School and Hospital of Stomatology, 22 Zhongguancun South Ave, 100081 Beijing, China.
Email: cora2005@126.com

Funding information

National Natural Science Foundation of China, Grant/Award Number: 81901029, 81700938 and 82001030; Natural Science Basic Research Program of Shaanxi, Grant/Award Number: 2020JQ-560; Xi'an "Science and Technology, Grant/Award Number: 20YXYJ0010(1); Fundamental Research Funds for the Central

Abstract

Objectives: Mammalian palatogenesis is a highly regulated morphogenetic process to form the intact roof of the oral cavity. Long noncoding RNAs (lncRNAs) and mRNAs participate in numerous biological and pathological processes, but their roles in palatal development and causing orofacial clefts (OFC) remain to be clarified.

Methods: Palatal tissues were separated from ICR mouse embryos at four stages (E10.5, E13.5, E15, and E17). Then, RNA sequencing (RNA-seq) was used. Various analyses were performed to explore the results. Finally, hub genes were validated via qPCR and in situ hybridization.

Results: Starting from E10.5, the expression of cell adhesion genes escalated in the following stages. Cilium assembly and ossification genes were both upregulated at E15 compared with E13.5. Besides, the expression of cilium assembly genes was also increased at E17 compared with E15. Expression patterns of three lncRNAs (*H19*, *Malat1*, and *Miat*) and four mRNAs (*Cdh1*, *Irf6*, *Grhl3*, *Efnb1*) detected in RNA-seq were validated.

Conclusions: This study provides a time-series expression landscape of mRNAs and lncRNAs during palatogenesis, which highlights the importance of processes such as cell adhesion and ossification. Our results will facilitate a deeper understanding of the complexity of gene expression and regulation during palatogenesis.



Universities, Grant/Award Number: xzy012020110; Shanghai Sailing Program, Grant/Award Number: 19YF1426400

KEYWORDS

lncRNAs, mRNAs, orofacial clefts, palatogenesis, RNA-seq

1 | INTRODUCTION

In mammals, the palate provides physical separation between the mouth and nasal cavity and thus plays essential roles in a wide array of physiological processes, including breathing, feeding, swallowing, speech, and hearing. Genetic or environmental factors that disrupt the palatogenesis often result in the cleft palate (CP), which is one of the most common craniofacial congenital deformities (Dixon et al., 2011; Martinelli et al., 2020). Approximately, the isolated CP affects 6.35 per 10,000 live births, and cleft lip with or without palate (CL/P) affects 10.63 per 10,000 live births (Parker et al., 2010). CP affects patients' quality of life even after surgical interventions and imposes a heavy burden on families and society. Hence, there is a great need for a better understanding of the regulatory mechanisms of palatal development.

Palatogenesis spans about 11 weeks in humans. In contrast, mouse palatogenesis is highly accelerated to approximately 8 days. Nevertheless, the palate development, anatomy, and function are strikingly similar in humans and mice, making the mouse an excellent model for understanding molecular and cellular mechanisms of palatogenesis. Briefly, palatogenesis involves the development of the primary and secondary palate. The primary palate is formed by the embryonic frontonasal prominence and contains the upper incisor region anterior to the incisive foramen. The secondary palate arises from bilateral palatal shelves derived from the maxillary prominences and constitutes the majority of the hard palate and the soft palate. In mice, secondary palate development is initiated on the embryonic Day 11.5 (E11.5) as the maxillary prominences outgrow internally to form the palatal shelves. From E12.5 to E13.5, the palatal shelves grow vertically on either side of the tongue, followed by elevation to their horizontal directions between E14 and E14.5. The palatal shelves then grow toward the midline and fuse with each other in an anterior-posterior sequence. The fusion starts at E14.5, and fusion of the hard palate is completed by E16.5 (Bush & Rulang, 2012; Li et al., 2019).

Therefore, palatal development involves several highly regulated morphogenetic processes, including palatal shelves growth, elevation, adhesion, and fusion. Although recent studies have provided new insights into the regulatory genes and pathways during these processes, the mechanisms underlying palatogenesis and palate defect remain elusive.

Long noncoding RNAs (lncRNAs) are generally described as RNA transcripts longer than 200 nucleotides (nt) that have no protein-coding potential (Dhamija & Diederichs, 2016). Emerging evidence shows that lncRNAs are associated with various cellular functions and play key roles in development (Ritter et al., 2019; Wang et al., 2019) and diseases (Bhan et al., 2017; Doan et al., 2016; Hong et al., 2020a). Studies of differentially expressed lncRNAs in all-trans

retinoic acid (ATRA) or 2,3,7,8-tetrachlorodibenzo-p-dioxin (TCDD)-treated mice have been conducted (Gao et al., 2017a, 2017b, 2020; Shu et al., 2019b). Studies on *Pax9* or *Tgf- β 3* mutant mice described the transcriptome profiles of wild-type and mutant mice palates from E13.5 or E14.5 to E16.5, respectively (Jia et al., 2017; Ozturk et al., 2013). However, none of the studies investigated the expression profiles of lncRNAs in normal mice embryos at the whole developmental stages of the mouse palate. Thus, relevant studies are still insufficient to gain a full understanding of the expression of lncRNAs during palatogenesis.

RNA sequencing (RNA-seq) is a high-throughput approach for genome-wide transcriptome quantification, including mRNAs and lncRNAs (Garber et al., 2011; Wang et al., 2009). Time-course experiments using RNA-seq technique can help uncover gene expression profiles during palatogenesis and identify significant genes and biological processes that regulate or characterize the developmental stages. In this study, we performed RNA-seq for palatal tissues at different time points throughout palatogenesis. The differentially expressed mRNAs and lncRNAs, as well as the pivotal biological processes and pathways with temporal characteristics, between stages, were unveiled. Expression patterns of three lncRNAs and four mRNAs detected in RNA-seq were validated.

2 | MATERIALS AND METHODS

2.1 | Samples

Mature ICR mice were purchased from Beijing Charles River Laboratories. The purchased animals were maintained in pathogen-free conditions with free access to the same food and water. The mice were raised in the standard cage under the 12/12 h light and dark cycle, 22–25°C room temperature, 55% \pm 10% relative humidity, and adequate ventilation. The cages were in corn cob bedding and nesting tissue for enrichment. Mice were mated, and the day when a vaginal plug was found was designated as Day 0 of pregnancy. On embryonic gestation Days 10.5 (E10.5), 13.5, 15 and, 17, the mice were chosen randomly and sacrificed by cervical dislocation. The embryos of the mice were isolated. Embryo mice were killed by decapitation. The heads of the embryonic mice were dissected in phosphate-buffered saline (PBS) under a dissecting microscope. We used the same batch of mice as well as the same reagent to control the confounding factors. For embryos at E10.5, the bilateral maxillary prominences were isolated. For the other time points, the mandible and the tongue were removed, and the palatal shelves were kept. Each embryo was from one individual pregnant mouse. The isolated palate specimens ($n = 3$ for each time point, 12 mouse embryos totally) were then treated with TRIzol reagent



(CoWin Bio.) and stored at -80°C . The animal study protocol was approved by the Committee on the Ethics of Animal Experiments of Peking University (permit number: LA2018192). The experiments were performed in strict accordance with the animal care and use guidelines. Criteria established for euthanizing animals before the planned end of the experiment were as follows: the investigators try to avoid their panic, reduce the pain of animals and struggle, shorten the death time, and pay attention to the safety of laboratory personnel. Cervical dislocation was used to euthanize mice. All sections of this study comply with the ARRIVE Guidelines for animal research and the completed ARRIVE 2.0 Guidelines checklist is attached as a supplemental file.

2.2 | Scanning electron microscopy (SEM)

For SEM, samples were dissected in $1\times$ PBS at room temperature and directly fixed in half-strength Karnovsky's fixative (2% PFA, 2.5% glutaraldehyde, 0.1 M cacodylate buffer) overnight or longer at 4°C . Then, we dehydrated them through an ethanol series. Samples were processed and observed according to standard procedures (Sulik et al., 1994). Samples were observed using Zeiss SUPRA 25 FESEM.

2.3 | RNA extraction, RNA-seq, and analysis of differentially expressed genes

Total RNA was extracted using an Ultrapure RNA Kit (CoWin Bio.) according to the manufacturer's protocol. Each sample went through verification for purity and integrity: $\text{RNA} \geq 10 \mu\text{g}$, concentration of $\text{RNA} \geq 100 \text{ ng}/\mu\text{l}$, $1.8 < \text{OD}_{260}/\text{OD}_{280} < 2.2$, $\text{OD}_{260}/\text{OD}_{230} \geq 2$, $28\text{S}/18\text{S} \geq 1$, RNA Integrity Number > 7.0 . The samples that met the guidelines were prepared according to the manufacturer's instructions (Epicentre Biotechnologies). After that, paired-end sequencing was performed using the Illumina HiSeq X Ten. After the quality filtering and trimming by Fastp (minLength = 50, BaseNLimit = 5, QualifiedQuality = 15), genes with low counts were filtered out and raw reads were trimmed and aligned to the mice GRCm38/mm10 reference database using Hisat2 (minIntronLen = 20, maxIntronLen = 500,000, trim5 = 5, trim3 = 5) (Chen et al., 2018; Kim et al., 2019). After alignment, lncRNAs and mRNAs were selected according to the gene type annotation information of NCBI Gene database (<https://www.ncbi.nlm.nih.gov>) and other RNAs were discarded. HTseq in union mode was used to analyze differential gene and transcript expression in RNA-seq experiments (Anders et al., 2015). The transcripts per kilobase transcriptome per million mapped reads (TPM) were calculated to assess the expression level of genes. Differentially expressed genes (DEGs) were detected using EBSseq of R package (v 1.16.0) based on the raw data (Leng et al., 2013). DEGs were defined based on two criteria: (i) fold changes ≥ 2 ; (ii) false discovery rate (FDR) < 0.05 .

2.4 | Quality control of the RNA-seq data

For RNA-seq, we constructed paired-end libraries and sequenced more than 1.02×10^8 reads per sample, with Q20 $> 97\%$ and Q30 $> 93\%$ on average. Then, the raw reads were filtered and mapped to the GRCm38/mm10 reference database. The mapping rates for all samples were greater than 94% (Table S1). The reads distribution on the chromosomes, as shown in Figure S1a, was approximately proportional to the chromosome length. Besides, the analysis of the gene structure revealed that the majority of the mapped reads were localized in the exon and intron regions (Figure S1b). To gain insights into the mRNA and lncRNA expression profiles at different embryonic gestation days, principal component analysis (PCA) and Spearman correlation analysis were performed. PCA on all expression genes (16,512 genes) detected by RNA-seq without filtering was conducted by princomp R package with default parameters. A high degree of similarity among E13.5, E15, and E17 was demonstrated by the multiple Spearman analyses ($R^2 \geq 0.948$) (Figure S1c).

2.5 | Functional enrichment analyses

Once the differentially expressed mRNA-related genes were identified, Gene Ontology (GO) and Kyoto Encyclopedia of Genes and Genomes (KEGG; <http://www.kegg.jp/>) analyses were performed to further understand the underlying biological functions and enriched pathways (p -value < 0.05) (Ashburner et al., 2000; Kanehisa & Goto, 2000, Consortium TGO, 2020).

2.6 | Weighted Gene Co-expression Network Analysis (WGCNA) and Short Time-Series Expression Miner (STEM) analysis

Weighted Gene Co-expression Network Analysis was conducted to describe the correlation patterns of different genes. All the DEGs were included to construct the co-expression network by R package WGCNA (Langfelder & Horvath, 2008). We set soft-thresholding power as twenty when the correlation coefficient was 0.8, and minimal module size as 30. Outliers in the clustering results were eliminated. Expression network data of correlated DEGs were obtained.

Short Time-Series Expression Miner analysis was a clustering algorithm to organize the transcription factors with various preset expression profiles over short time-series (Ernst et al., 2005). Gene expression values were transferred to log ratios relative to E10.5. Then, the values of each gene were assigned to the algorithm to match the criteria of one of the predefined expression model profiles. Standard hypothesis testing was used. The correlation coefficient, as well as the p -value using the actual assigned gene number of one profile and the expected assigned gene number, was determined (adjusted p -value, 0.05 by Bonferroni correction). The MaxProfile setting was 500 and the setting of Maximum Unit Change between

Time Points was 1. If the profiles are statistically significant, the box would be colored.

2.7 | Path-Act and Gene-Act Network Analyses

After obtaining the pathway annotations of the DEGs using KEGG databases, core differential pathways between stages and their interactions were identified via Pathway-Act Network analyses, as described previously (Li et al., 2015). In addition, with regard to the KEGG analyses, one differential gene could be mapped to multiple pathways, and could interact with several other genes. Therefore, Gene-Act Network was constructed to clarify the gene-gene interactions and key transcriptomic factors during palatogenesis. Briefly, the adjacency matrix was constructed after obtaining the interaction relationship between genes based on KEGG.

2.8 | lncRNA target prediction

The target genes of differentially expressed lncRNAs via cis-regulatory effects were identified by Miranda (Score: 150, Energy: -20) and RNAhybird (MaxTarget: 2,000,000, MaxQueryLen: 50, Energy: -25, HitsPerTarget: 1) (Enright et al., 2003; Rehmsmeier et al., 2004). Then, the intersection results of the two tools were selected. Then, with the help of the UCSC genome browser (<http://genome.ucsc.edu/>), we used ncRNA Location Analysis to ensure the position of identified lncRNA. The genes transcribed upstream or downstream of lncRNAs within a 10 kbp window were reckoned as potential cis target genes.

2.9 | Real-time quantitative PCR (qPCR)

The qPCR was performed to validate the result of RNA-seq. The protocol of extraction and verification for purity and integrity of total RNA was the same as what was described above. The qualified RNA was used to perform the reverse transcription-PCR to synthesize cDNA by using PrimeScript™ II 1st Strand cDNA Synthesis Kit (Takara Bio) according to the manufacturer's instructions. Then, we used 20 µl reaction system for qPCR, including 10 µl FastStart Universal SYBR Green Master Mix 2X (Roche Bio), 0.5 µl forward primer, 0.5 µl reverse primer, 7 µl RNase-free water, and 2 µl template cDNA. The reaction condition was as follows: 95°C for 10 min, followed by 40 cycles of 95°C for 15 s, 60°C for 1 min; 60–95°C melting curve. Using $2^{-\Delta\Delta Ct}$ method, the expression of the targeted genes was normalized to *Gapdh*. The primers used in qPCR experiments were listed in Table S2. Each PCR reaction had three repeats.

2.10 | Fluorescence in situ hybridization (FISH)

Embryos harvested at specific stages were dissected and then were fixed in fresh 4% paraformaldehyde overnight at 4°C. Next,

the samples were dehydrated in ethanol, embedded in paraffin, and sectioned at 4 µm. After deparaffinization, heat pretreatment, and protease treatment, the slides were prehybridized (37°C, 1 h) and hybridized (37°C, overnight) in probes. The post-hybridization step was processed by washing the slides in saline-sodium citrate buffer. Then, the slides were counterstain in DAPI for 8 min within a dark room and mounted in the antifade mounting medium. The slides were evaluated by using the fluorescence microscope. The probe information was listed in Table S3.

2.11 | Statistical analysis

All data are shown as mean ± standard deviations (SD) along with the 95% confidence intervals (CIs). Except for the analysis of qPCR, significant differences among groups were determined using the negative binomial distribution method for significant analysis (Ilott et al., 2014). *p*-value < 0.05 was considered statistically significant. All analyses were performed using SPSS 20.0 software (IBM).

3 | RESULTS

3.1 | Morphology and electron micrographs of embryonic palatal shelf tissue

The development stages of the secondary palate in mice were depicted in Figure 1a. We took SEM images of palatal samples at different stages of mouse embryos. At E10.5, the frontonasal prominence is divided into the medial and lateral nasal prominences by the formation of nasal pits. The maxillary prominences will outgrow to form the presumptive palatal shelves (Figure 1b). After their initiation at E11.5, the palatal shelves already exhibit clear shapes along the A-P axis and are about to reorient to a horizontal direction at E13.5 (Figure 1c). At E15, the palatal shelves meet at the midline and initiate the fusion process (Figure 1d). By E17, the fusion has completed, and the secondary palate has formed (Figure 1e).

3.2 | Differential expression analyses compared with E10.5

To identify the major shifts in the mRNA and lncRNA transcriptomes of the developing palate, we compared the expression profiles of specimens at later time points with that at E10.5, which is prior to the emergence of the mouse palate. Overall, the upregulated and downregulated numbers of mRNAs and lncRNAs were presented (Figure 2a). The upregulated genes were most enriched in the cell adhesion process (Figure 2b–d).

The pairwise comparison of lncRNA expression patterns revealed that when the palatal shelves experience initiation and rapid outgrowth (from E10.5 to E13.5), 914 lncRNAs were upregulated, and 701 lncRNAs were downregulated (Figure S2a). At E15, 942

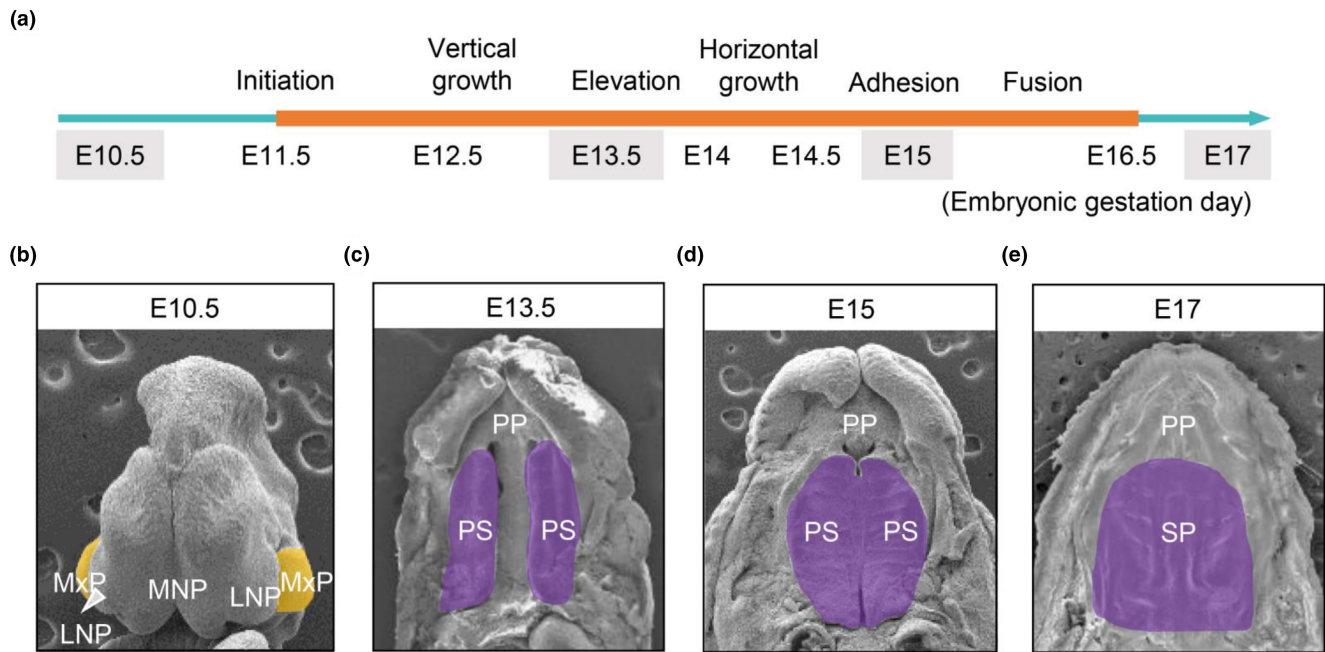


FIGURE 1 Morphology of the samples and summary of the RNA-seq data. (a) Time course of morphogenetic process of palate development in mice. (b) Scanning electron micrographs (SEM) showing the facial prominences at E10.5 in the coronal plane. The bilateral maxillary prominences (colored in yellow) that will give rise to the palatal shelves are dissected for RNA-seq. (c–e) SEM images showing oral views of the palate at representative stages. The tissues colored in purple were dissected for sequencing use. Scale bars are not equivalent between stages. LNP, lateral nasal prominence; MNP, medial nasal prominence; MxP, maxillary prominence; PP, primary palate; PS, palatal shelf; SP, secondary palate. The time points in (A) referred to Bush and Jiang (2012)

upregulated and 815 downregulated lncRNAs were detected compared with E10.5 (Figure S2b). At E17, 1,660 lncRNAs were upregulated, and 979 lncRNAs were downregulated (Figure S2c).

3.3 | Differential expression analyses between E15 and E13.5

From E13.5 to E15, the palatal shelves grow horizontally and start to adhere to each other at the midline. During this period, 692 and 32 mRNAs were detected to be upregulated and downregulated, respectively (Figure 2a). Meanwhile, there were 66 upregulated lncRNAs and 42 downregulated lncRNAs (Figure S3a). The predominant biological process was cilium movement (Figure 2e). Genes associated with related processes, including cell projection organization, outer dynein arm assembly, and motile cilium assembly, were all upregulated during this period. Cell adhesion was still crucial, and genes associated with pathways including ECM-receptor interaction and focal adhesion were upregulated (Figure 2f). Genes associated with ossification and biomineral tissue development were also upregulated.

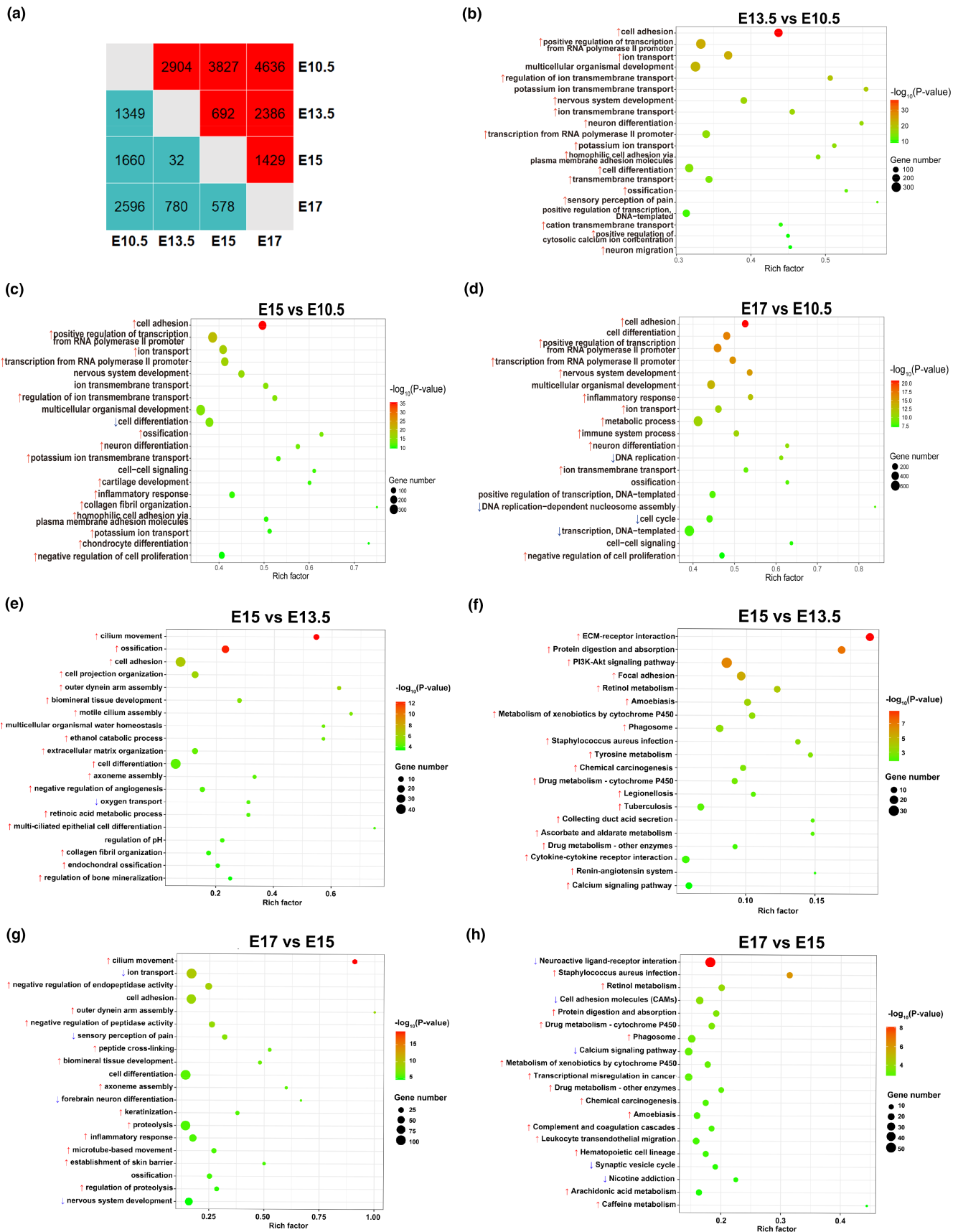
3.4 | Differential expression analyses between E17 and E15

The palatal fusion is initiated at E15 and completed by E16.5. The DEGs of the matured palate at E17 included 1,429 upregulated

and 578 downregulated mRNAs (Figure 2a). In addition, 446 lncRNAs were upregulated, and 87 lncRNAs were downregulated (Figure S3b). Genes associated with cilium movement were upregulated (Figure 2g). KEGG analysis showed that the genes were predominantly linked to downregulated neuroactive ligand-receptor interactions (Figure 2h).

3.5 | Correlation analysis, expression pattern, and target predictions

Weighted Gene Co-expression Network Analysis was performed to determine the correlation patterns of all the different expression genes detected by RNA-seq and EBSeq (12,209 genes). All differentially expressed lncRNAs and differentially expressed mRNAs were included in this analysis. The co-expression genes with high correlations were clustered into the same module, while the genes without correlation with other genes were eliminated. Ten different color modules representing ten different networks of correlated co-expression mRNAs and lncRNAs were obtained in this study (Figure 3). Gene statistics in each module were presented in Table S4. The module comprising most genes was the turquoise one (asterisk), which contained 6,007 genes. There were several hub genes relating to palatal development. This turquoise module (asterisk) contained mRNAs including *Cdh1*, *Irf6*, *Grhl3*, and lncRNAs including *H19* and *Malat1*, revealing the potential correlation of these DE-mRNAs and DE-lncRNAs (Figure 3). *Miat* was in the blue module while *Efnb1*



could not fit in any modules in the analysis (Figure 3). In addition, STEM analysis of transcription factors in DEGs was conducted to unveil the possible genes expression profiles (Figure S4). Temporal

expression patterns of transcription factors in DEGs were assessed and were fitted into different predefined model profiles, representing different sets of correlated transcriptional factors. Within the



FIGURE 2 Differential expression analyses of mRNAs and lncRNAs among E10.5, E13.5, E15, and E17. (a) The number of mRNAs that were significantly upregulated (red brackets) and downregulated (blue brackets) across stages. (b–d) GO analyses of the DEGs across stages. The biological processes marked with an up arrow are significantly upregulated (p -value < 0.05), and vice versa. If one biological process is not marked with an arrow, it means that some DEGs belonging to this process were significantly upregulated, while the others were downregulated. GO analysis of differential expression analyses between consecutive stages (e and g) and KEGG pathway analysis (f and h) of the DEGs between E15 versus E13.5 (e and f) and E17 versus E15 (g and h)

FIGURE 3 Weighted Gene Co-expression Network Analysis construct. The lower colorful rectangle represents different co-expression modules. Ten colors in all indicated that all the DEGs with correlations were classified as ten correlation expression patterns

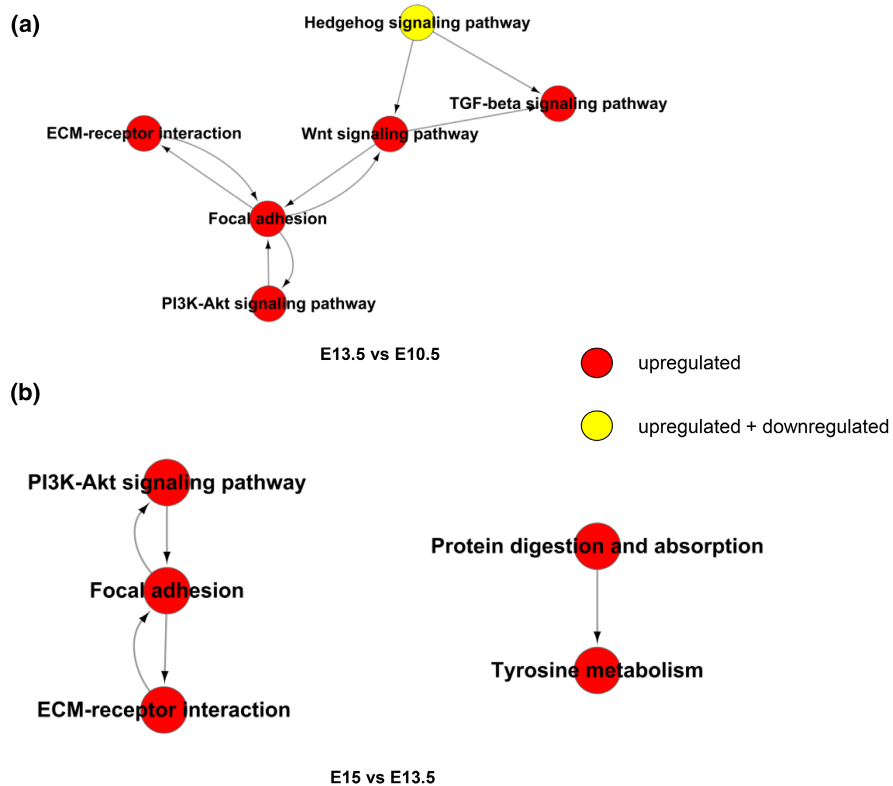
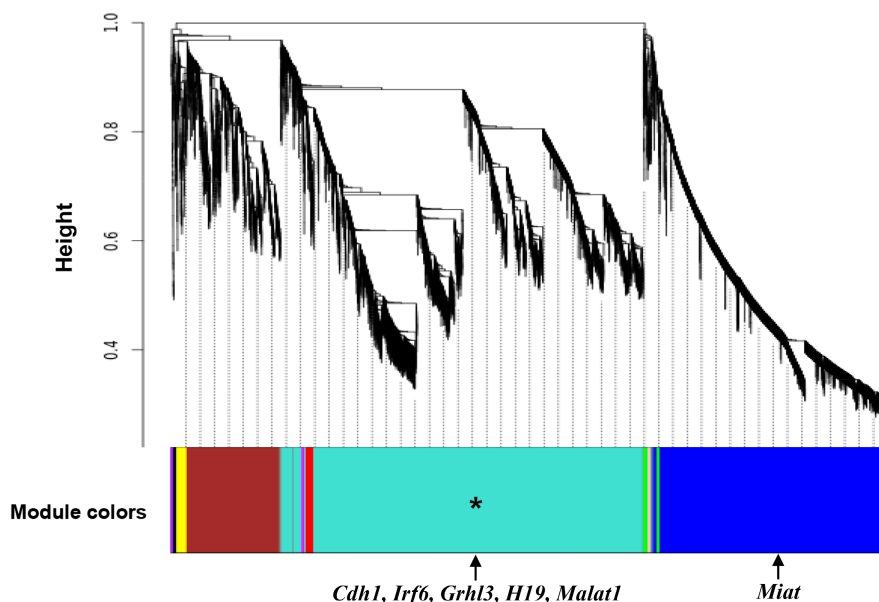


FIGURE 4 Pathway-Act Network exhibiting the interaction of selected differential pathways between consecutive stages. Red dots represent upregulated pathways. Yellow dots represent the pathways with both up- and down-regulated DEGs

25 model profiles, ten of them were statistically significant, which suggested that these ten sets of genes potentially affect the development of palates. All the profiles and related genes were presented in Table S5.

The top ten upregulated and downregulated lncRNA, as well as mRNA, in E10.5 versus E13.5, E13.5 versus E15, and E15 versus E17, were listed in Tables S6 and S7. We conducted a target prediction for significant lncRNAs to explore potential cis target genes by Miranda and RNAhybrid. Genes transcribed upstream or downstream of lncRNAs within a 10 kbp window were predicted as potential targets. In total, 17 lncRNAs were suggested to have 23 potential cis targets (Table S8). There were two DEGs in the 23 potential targets, while in E13.5 versus E15, 16,512 expression genes contained 722 non-target DEGs. Thus, the potential target genes changed more frequently (containing 8.70% DEGs) than non-target genes (containing 4.37% DEGs) in the critical period (E13.5–E15) of palatogenesis. According to WGCNA, nine lncRNAs were probably correlated with the cis targets in terms of expression changes.

We recruited the DEGs of lncRNA from E13.5 versus E10.5, E15 versus E13.5, and E17 versus E15. A total of 2,256 lncRNAs were obtained. We reviewed all the lncRNAs in the literature to figure out the lncRNAs associated with mammalian palatogenesis. Surprisingly, only three lncRNAs (*H19*, *Meg3*, and *Xist*) have been known to be associated with mammalian palatogenesis (Gao et al., 2017b; Liu et al., 2021; Yeung et al., 2014). According to the analyses in this study, we propose that biological processes including adhesion, cilia, and bone-related process are important in palatal development. Thus, to narrow down the range, we used a web crawler tool in our previous study (Zhong et al., 2021) to review all the DE-lncRNAs in NCBI (<https://pubmed.ncbi.nlm.nih.gov/>) and discovered 22 lncRNAs (including *H19*, *Meg3*, and *Xist*) associated with the above-mentioned processes, which are potential lncRNAs that may affect mammalian palatogenesis (Table S9).

3.6 | Pathway Interactions and gene interaction network analysis

Top-ranked pathways in KEGG analysis were analyzed by Path-Act Network to clarify pathway interactions. PI3K-Akt, focal adhesion, ECM-receptor interaction, WNT, and TGF- β pathways were more active at E13.5 compared with E10.5 (Figure 4a). Upregulation and downregulation were witnessed in the Hedgehog pathway. PI3K-Akt, focal adhesion, ECM-receptor interaction, protein digestion and absorption, and tyrosine metabolism were more active at E15 compared with E13.5 (Figure 4b). When it came to E17 versus E15, no significant pathway in KEGG was identified (Figure S5). The pathway analysis suggested that cilium-related pathways (Hedgehog, WNT, and TGF- β pathways) and cell-adhesion-related pathways (focal adhesion pathway) might be pivotal in palatal development.

To clarify the gene-gene interactions and key transcription factors during palatogenesis, we conducted the Gene-Act Network analysis based on KEGG analysis. Both analyses of E13.5 versus

E10.5 and E17 versus E15 suggested that the nuclear hormone receptor family may be one of the cores in the gene-gene interaction network (Figure 5a,b). Besides, the STAT family, the WNT family, the forkhead box O protein family, and the nuclear factor of activated T cells family were part of the cores in the network of E13.5 versus E10.5 (Figure 5b). However, analysis in E15 versus E13.5 revealed no significant TF-related interactions (Figure S6).

3.7 | Validation of RNA-seq

We selected three lncRNAs (*H19*, *Malat1*, and *Miat*) and four mRNAs (*Cdh1*, *Irf6*, *Grhl3*, and *Efnb1*) for qPCR analysis at E10.5, E13.5, E15, and E17 to validate the results of RNA-seq. *H19* is known as a cleft palate related gene. *Malat1* and *Miat* might be potentially related to the development of the palate. In addition, these three genes have high expression levels and significant expression differences among the four time points. *Cdh1*, *Irf6*, *Grhl3*, and *Efnb1* were adhesion-related genes. Furthermore, the correlation of mRNAs including *Cdh1*, *Irf6*, *Grhl3*, and lncRNAs including *H19* and *Malat1* was indicated by WGCNA. The expression patterns of the detected genes were consistent with the RNA-seq data (Figure 6A–G), which validated the results of RNA-seq.

We also performed FISH for the three lncRNAs in the palatal tissue section of E10.5 and E15 mice (Figure S7). For *Malat1* and *H19*, the E15 sections suggested more expression than that of E10.5. When it comes to *Miat*, the E10.5 section exhibited obviously more expression compared with the E15 section. The results were consistent with the RNA-seq results.

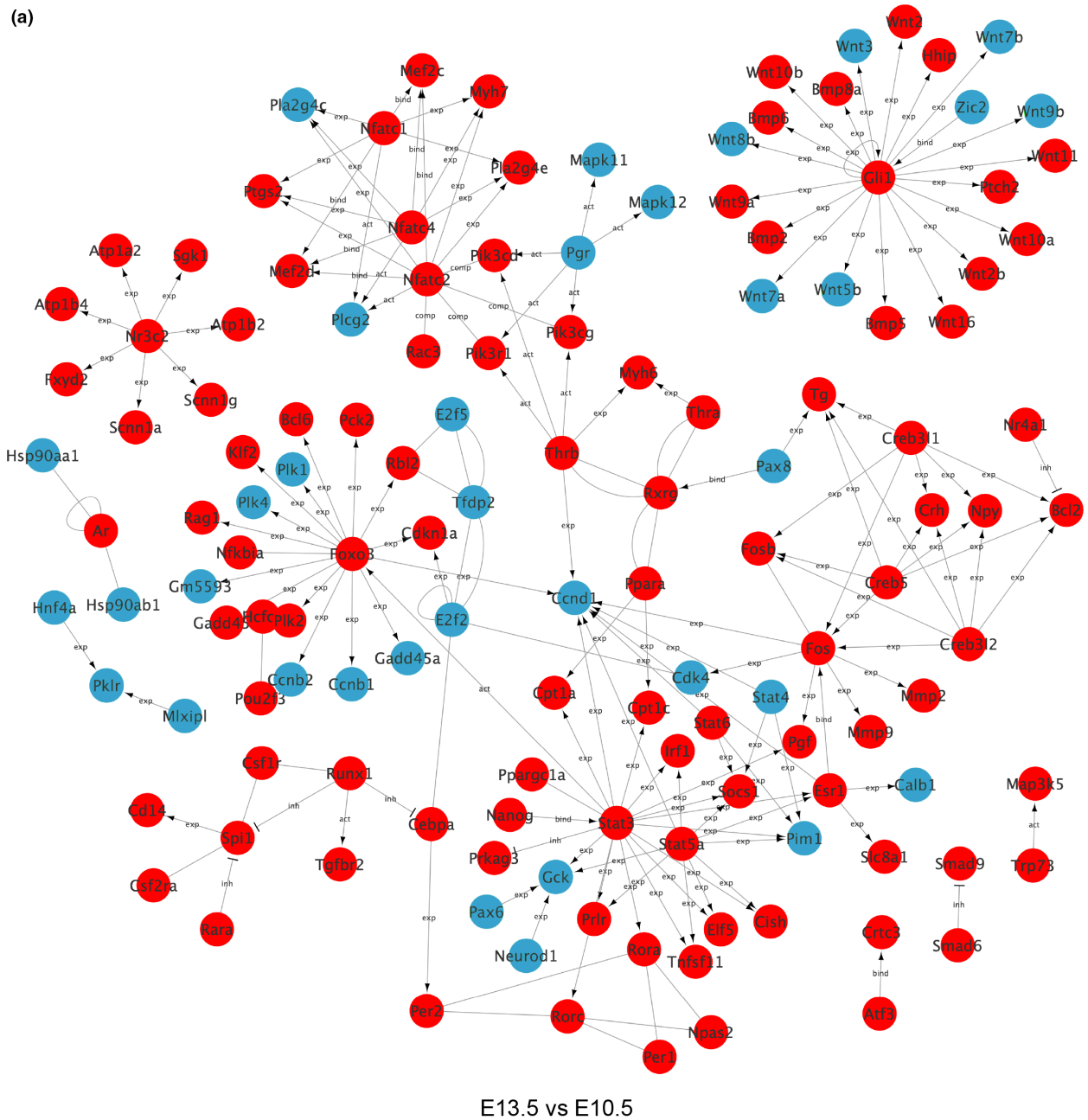
4 | DISCUSSION

Mammalian palatogenesis is a morphogenetic process that is precisely controlled by a gene-regulatory network. Even minor alterations in this intricate network may cause CP, one of the most common congenital birth defects in humans. A comprehensive mRNAs and lncRNAs expression profile across all palatal developmental stages can reveal the enormous diversity in gene expression and its stage-specific regulation. In this study, our RNA-seq analysis on mice provides the gene expression divergence among different palatogenesis stages. The functional characterization of mRNAs, lncRNAs, and pathways underlying the divergence can further facilitate the understanding of the molecular basis of palatogenesis.

Evidence has shown that lncRNAs are instrumental for gene regulation during palatal development (Jarroux et al., 2017; Yun et al., 2019), as recent studies in all-trans retinoic acid-induced CP mice have revealed that lncRNAs play key roles in the epithelial-mesenchymal transition (EMT) process during palatal fusion (Gao et al., 2017a; Shu et al., 2019a, 2019c). Moreover, lncRNA *H19* is associated with cleft palate and the development of palate (Gao et al., 2017a, 2017b). *Miat* affects osteogenic differentiation and vascular growth by regulating vascular endothelial growth factor



(a)



(b)

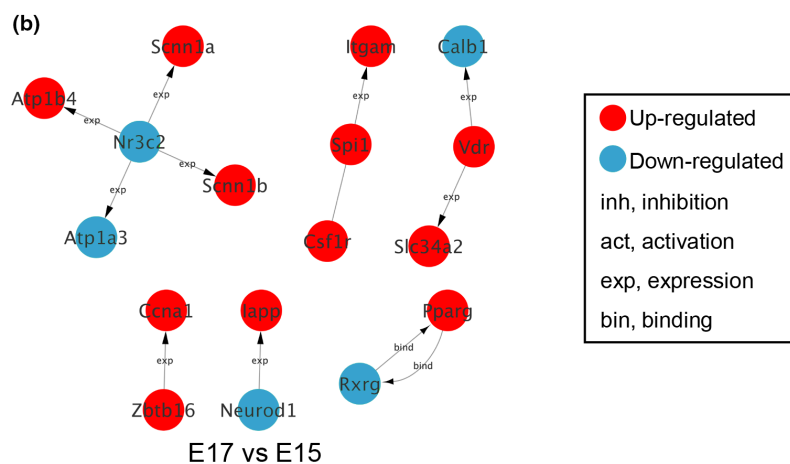


FIGURE 5 Gene-Act Network of DEGs at E13.5 versus E10.5 and E17 versus E15. Red and blue dots represent up- and down-regulated genes. The arrows indicate the connections and regulatory relationships between two genes

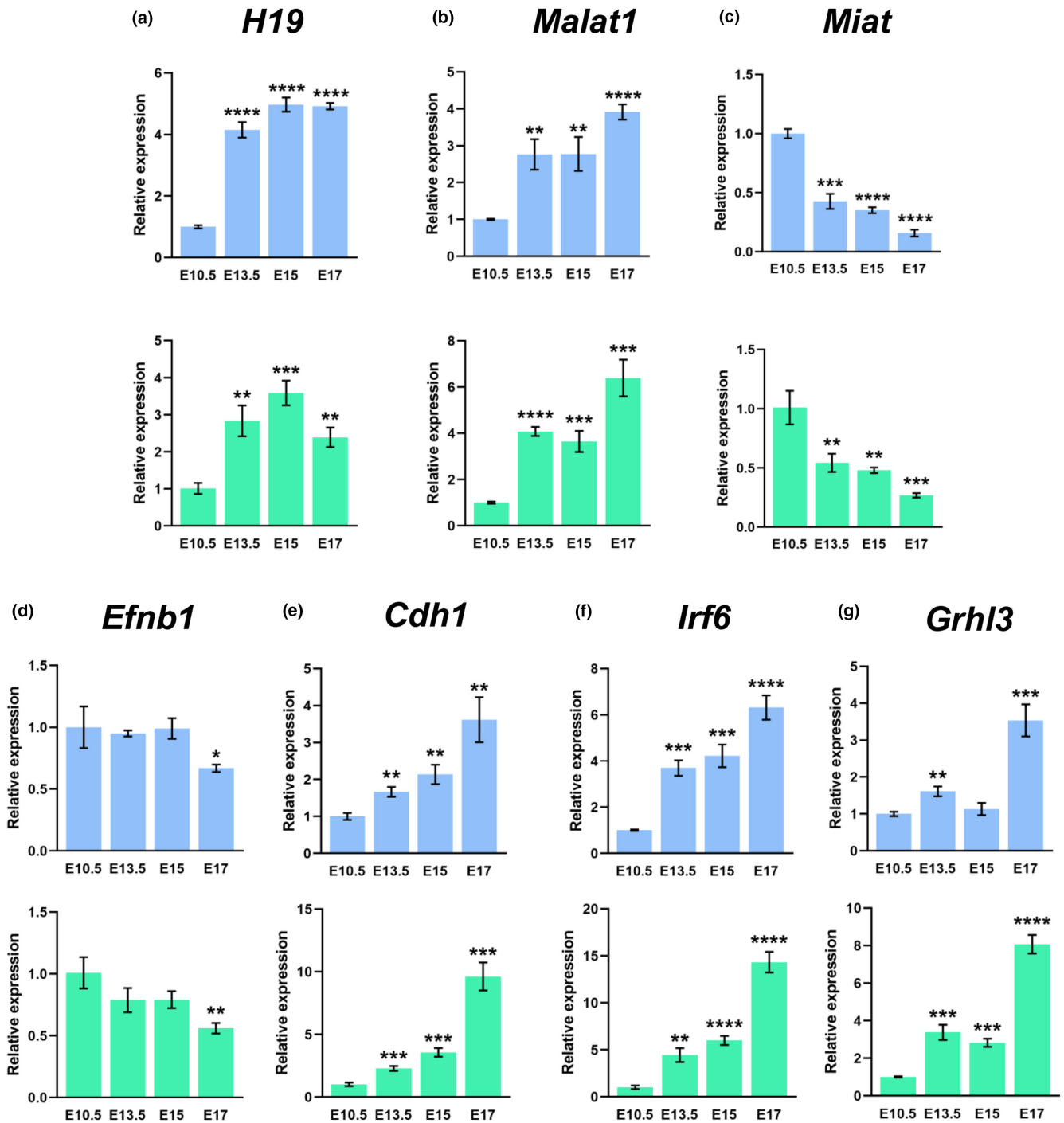


FIGURE 6 qPCR validation of RNA-seq data. (a–c) Relative expression levels of lncRNA by RNA-seq and qPCR. (d–g) Relative expression levels of mRNA by RNA-seq and qPCR. The upper blue panels represent the TPM data of RNA-seq and the lower green panels represent the data of qPCR. * $p < 0.05$, ** $p < 0.01$, *** $p < 0.001$, **** $p < 0.0001$

(VEGF), the vital factor associated with the etiology of cleft palate (Hong et al., 2020b; Jin et al., 2017). *Malat1* regulates bone differentiation and might affect the development of bone in the palate (Hong et al., 2020b).

Some abundant lncRNAs (e.g., *H19* and *Malat1*) can function as post-transcriptional regulators via sponging microRNAs (miRNAs) (Statello et al., 2021), thereby repressing crucial miRNAs availability

to silence mRNAs during palatogenesis. Several such miRNAs have been reviewed recently (Schoen et al., 2017). In this study, the *H19* lncRNA expression increased during palatal initiation and outgrowth phases (E10.5 – E13.5 and E13.5 – E15) and decreased to some extent at E17 (Figure 6). Expression of miR-17-92 cluster, key regulators of palatal shelves (PS) outgrowth, and bone formation (Wang et al., 2013; Zhou et al., 2014) was reported to decrease



from E12 to E14 in the murine PS (Mukhopadhyay et al., 2010). Given that miR-17-92 cluster has been shown to be counteracted by *H19* in various tumor cells (Li et al., 2020), it is plausible to conclude that the downregulation of miR-17-92 cluster was mediated by *H19* during this phase of palatogenesis. Closer investigation of the effect of different *H19* expression levels on the expression profiles of miR-17-92 cluster and its critical targets, including BMP (Ning et al., 2013), Hedgehog (Uziel et al., 2009), and TGF- β signaling pathways (Li et al., 2012) would help understand palatogenesis. Apart from *H19*, the expression of another significant lncRNA, *Malat1*, increased from E10.5 to E13.5 after which it leveled off, and increased again in the last phase of palatogenesis, that is, palatal fusion. The second increase of *Malat1* expression may be responsible for the reported decrease of miR-200b (Shin et al., 2012a), which orchestrates palatal fusion (Shin et al., 2012b), considering that the sequestering of miR-200b by *Malat1* has been identified in tumors (Fan et al., 2020). However, the interactions between miRNAs, lncRNAs and their functional outcomes in palatogenesis await further elucidation.

We also sought to characterize the mRNA transcriptional profiles of the presumptive PS at E10.5 in comparison with that of the PS tissues at follow-up time points (E13.5, E15, and E17). The mRNA expression profile changed drastically after the initiation of palatogenesis but showed a considerable degree of similarity during development. Compared with E10.5, the genes related to cell adhesion were upregulated, and cell adhesion was the most enriched biological process. The critical role of adhesion in palatal development was most discussed in the palatal closure process (Li et al., 2019), the molecular basis of which has been reviewed recently (Lough et al., 2017). As the palatal shelves grow horizontally toward each other, adhesion of the medial edge epithelia (MEE) takes place and then the medial epithelial seam (MES) forms, whose dissolution initiates the fusion process. Mutations in several genes encoding epithelial adhesion proteins have been identified to be causative for cleft lip with or without palate (CL/P) in humans, such as adherence junction proteins *NECTIN1* (Nectin-1), *EFNB1* (ephrin-B1), and *CDH1* (E-Cadherin) (Cox et al., 2018; Vogelaar et al., 2013). In our study, *Cdh1* was upregulated over time. Apart from that, it is noteworthy that adhesion proteins and regulatory transcriptional factors (such as *Irf6* and *Grhl* family genes) were also upregulated at the earlier stage (E13.5). During this period, the vertically growing palatal shelves are in contact with the mandibular and lingual epithelia, and the prevention from pathological fusions between the palate and the mandible/tongue is mediated by the periderm (Hammond et al., 2019; Richardson et al., 2014), which exhibits a highly polarized expression of cell adhesion complexes. Taken together, cell adhesion plays essential roles in mediating tissue integrity (Priest et al., 2017) and in palate morphogenesis throughout the process. Hence, we selected *Efnb1*, *Cdh1*, *Irf6*, and *Grhl3* to verify the RNA-seq using qPCR.

As palatogenesis is a process with distinct temporal characteristics, we further analyzed the difference of transcriptional expression profiles between consecutive stages E15 versus E13.5 and E17

versus E15. Differential expression analysis of E15 versus E13.5 revealed the significance of ECM during the growth and elevation of palates, which were in accord with the results of a previous study on all-trans retinoic acid induced cleft palate of mice (Peng et al., 2020). According to the GO analyses and KEGG analyses, DEGs linked to primary ciliary assembly and function were upregulated, demonstrating their importance during palatal development. The primary cilium is a pivotal sensory organelle acting as a major signaling hub for a number of signaling pathways that are essential for craniofacial development, such as Hedgehog (Briscoe & Théron, 2013; De Mori et al., 2017; Nandadasa et al., 2019) and WNT (Yuan et al., 2017) signaling. Dysfunction of cilium disrupts multiple signaling pathways and their interactions, resulting in widespread phenotypic defects, collectively termed as ciliopathies (Waters & Beales, 2011). The most common palatal defects reported in ciliopathies include high arched palate or CLP, characterized in Joubert Syndrome (Halbritter et al., 2013), Meckel-Gruber Syndrome (Barker et al., 2014), and Oral-Facial Digital Syndromes (Thauvin-Robinet et al., 2014).

It is noteworthy that a study on the transcriptome of *Tgf- β 3* mutant mice identified eight genes that were all overlaid with TGF- β signaling, possibly contributing to the cleft palate (Ozturk et al., 2013). Another study on the wild-type and *Pax9* mutant mice indicated the importance of PAX9-dependent WNT signaling in palatogenesis, suggesting that the WNT agonist injected into *Pax9*^{+/-} mice during critical gestation windows may restore the cleft palate of embryonic mice (Jia et al., 2017). In line with the studies mentioned above, Path-Act analysis in our study implied that Hedgehog, WNT, and TGF- β pathways interacted directly during the early stage of palatal development. WNT signaling also interacted with the focal adhesion process, indicating that cilium movement might be associated with cell adhesion.

Gene-Act network and pathway analysis unveiled several core gene families, some of which have proved to affect palatal development, such as *Stat3* (Hall et al., 2017) and *Wnt9a* (Dougherty et al., 2013). Therefore, other genes in these families might be key nodal genes in the development of the palate, which required further investigations in the future.

There are some limitations to this study. First of all, there are insufficient annotations of lncRNAs to conduct some further analysis. As increasing numbers of studies in lncRNAs were published, this problem should be solved gradually. Second, our bioinformatics analysis requires further molecular experiments and animal models to confirm its physiological significance in future studies. Furthermore, as we know, the epithelial and mesenchymal cells play different roles in the development of palate (Li et al., 2017); thus, bulk RNA-seq used in this study could not distinguish results from epithelial and mesenchymal tissues, which is a limitation of our study. However, as suggested by some previous studies, bulk RNA-seq is an effective strategy and could identify the most significant hub genes and key pathways, giving clues for later research (Jia et al., 2017; Ozturk et al., 2013). In addition, since there are some pathways involved interactions between epithelium and mesenchyme such as SHH or WNT (Maimets et al., 2022; Sarkar

et al., 2000), sequencing for the mixture tissue will not conceal the possible interactions involving the two different tissues. In the future, some new techniques such as high-precision micromanipulation or single-cell sequencing could be applied to give us more precious and insightful evidence.

In brief, we characterized the mRNAs and lncRNAs transcripts with regard to different stages of palatogenesis. Pathway and gene interaction analyses were conducted to identify potential core regulation processes such as cell adhesion, ossification, as well as the significant genes such as *H19*, *Malat1*, *Cdh1*, *Irf6*, and *Ghrh3*. This study enhances the understanding of palatogenesis regulation and etiology of cleft palate, which provides a substantial resource to the palatal development research community.

ACKNOWLEDGEMENT

This study was supported by fundings from the National Natural Science Foundation of China (No. 81901029, No. 81700938, and No. 82001030), the Natural Science Basic Research Program of Shaanxi (No. 2020JQ-560), Xi'an "Science and Technology+" Action Plan-Medical Research Project (No. 20YXYJ0010(1)), the Fundamental Research Funds for the Central Universities (No. xzy012020110), Shanghai Sailing Program (No. 19YF1426400). The funding bodies had no role in the study design, data collection and interpretation, decision to publish, or in writing the manuscript.

CONFLICT OF INTEREST

The authors declare that they have no conflicts of interest.

AUTHOR CONTRIBUTIONS

Wenbin HUANG: Data curation; Investigation; Methodology; Software; Validation; Visualization; Writing – original draft. **Wenjie Zhong:** Data curation; Formal analysis; Investigation; Writing – original draft. **Qing He:** Data curation; Methodology; Software. **Yizhu Xu:** Formal analysis; Investigation; Validation. **Jiuxiang LIN:** Methodology; Resources; Writing – review & editing. **Yi Ding:** Methodology; Writing – review & editing. **Huaxiang Zhao:** Conceptualization; Funding acquisition; Project administration; Supervision; Writing – review & editing. **Xiaowen Zheng:** Conceptualization; Funding acquisition; Resources; Supervision; Writing – review & editing. **Yunfei Zheng:** Conceptualization; Funding acquisition; Methodology; Project administration; Resources; Supervision; Writing – review & editing.

PEER REVIEW

The peer review history for this article is available at <https://publons.com/publon/10.1111/odi.14237>.

DATA AVAILABILITY STATEMENT

Differentially expressed genes (DEGs) are available at China National GeneBank DataBase (<https://db.cngb.org/>), with accession number: [CNX0438826](https://db.cngb.org/record/CNX0438826). More additional information are available from the corresponding author Dr. Huaxiang Zhao (huaxiangzhao@xjtu.edu.cn) on reasonable request.

ORCID

Huaxiang Zhao  <https://orcid.org/0000-0002-9661-0166>

Yunfei Zheng  <https://orcid.org/0000-0003-1899-8051>

REFERENCES

- Anders, S., Pyl, P. T., & Huber, W. (2015). HTSeq—A Python framework to work with high-throughput sequencing data. *Bioinformatics (Oxford, England)*, *31*, 166–169.
- Ashburner, M., Ball, C. A., Blake, J. A., Botstein, D., Butler, H., Cherry, J. M., Davis, A. P., Dolinski, K., Dwight, S. S., Eppig, J. T., Harris, M. A., Hill, D. P., Issel-Tarver, L., Kasarskis, A., Lewis, S., Matese, J. C., Richardson, J. E., Ringwald, M., Rubin, G. M., & Sherlock, G. (2000). Gene ontology: Tool for the unification of biology. The gene ontology consortium. *Nature Genetics*, *25*, 25–29.
- Barker, A. R., Thomas, R., & Dawe, H. R. (2014). Meckel-Gruber syndrome and the role of primary cilia in kidney, skeleton, and central nervous system development. *Organogenesis*, *10*, 96–107.
- Bhan, A., Soleimani, M., & Mandal, S. S. (2017). Long noncoding RNA and cancer: A new paradigm. *Cancer Research*, *77*, 3965–3981.
- Briscoe, J., & Théron, P. P. (2013). The mechanisms of Hedgehog signalling and its roles in development and disease. *Nature Reviews Molecular Cell Biology*, *14*, 416–429.
- Bush, J. O., & Rulang, J. (2012). Palatogenesis: Morphogenetic and molecular mechanisms of secondary palate development. *Development*, *139*, 231–243.
- Chen, S., Zhou, Y., Chen, Y., & Gu, J. (2018). fastp: An ultra-fast all-in-one FASTQ preprocessor. *Bioinformatics (Oxford, England)*, *34*, i884–i890.
- Consortium TGO (2020). The gene ontology resource: Enriching a Gold mine. *Nucleic Acids Research*, *49*, D325–D334.
- Cox, L. L., Cox, T. C., Moreno Uribe, L. M., Zhu, Y., Richter, C. T., Nidey, N., Standley, J. M., Deng, M., Blue, E., Chong, J. X., Yang, Y., Carstens, R. P., Anand, D., Lachke, S. A., Smith, J. D., Dorschner, M. O., Bedell, B., Kirk, E., Hing, A. V., ... Roscioli, T. (2018). Mutations in the epithelial cadherin-p120-catenin complex cause mendelian non-syndromic cleft lip with or without cleft palate. *American Journal of Human Genetics*, *102*, 1143–1157.
- De Mori, R., Romani, M., D'Arrigo, S., Zaki, M. S., Loreface, E., Tardivo, S., Biagini, T., Stanley, V., Musaev, D., Fluss, J., Micalizzi, A., Nuovo, S., Illi, B., Chiapparini, L., Di Marcotullio, L., Issa, M. Y., Anello, D., Casella, A., Ginevrino, M., ... Valente, E. M. (2017). Hypomorphic recessive variants in *SUFU* impair the sonic hedgehog pathway and cause joubert syndrome with cranio-facial and skeletal defects. *American Journal of Human Genetics*, *101*, 552–563.
- Dhamija, S., & Diederichs, S. (2016). From junk to master regulators of invasion: lncRNA functions in migration, EMT and metastasis. *International Journal of Cancer*, *139*, 269–280.
- Dixon, M. J., Marazita, M. L., Beaty, T. H., & Murray, J. C. (2011). Cleft lip and palate: Understanding genetic and environmental influences. *Nature Reviews Genetics*, *12*, 167–178.
- Doan, R. N., Bae, B. I., Cubelos, B., Chang, C., Hossain, A. A., Al-Saad, S., Mukaddes, N. M., Oner, O., Al-Saffar, M., Balkhy, S., Gascon, G. G., Nieto, M., & Walsh, C. A. (2016). Mutations in human accelerated regions disrupt cognition and social behavior. *Cell*, *167*, 341–354.e12.
- Dougherty, M., Kamel, G., Grimaldi, M., Gfrerer, L., Shubinets, V., Ethier, R., Hickey, G., Cornell, R. A., & Liao, E. C. (2013). Distinct requirements for *wnt9a* and *irf6* in extension and integration mechanisms during zebrafish palate morphogenesis. *Development*, *140*, 76–81.
- Enright, A. J., John, B., Gaul, U., Tuschl, T., Sander, C., & Marks, D. S. (2003). MicroRNA targets in drosophila. *Genome Biology*, *5*, R1.
- Ernst, J., Nau, G. J., & Bar-Joseph, Z. (2005). Clustering short time series gene expression data. *Bioinformatics (Oxford, England)*, *21*, i159–i168.



- Fan, L., Huang, X., Chen, J., Zhang, K., Gu, Y. H., Sun, J., & Cui, S. Y. (2020). Long noncoding RNA MALAT1 contributes to sorafenib resistance by targeting miR-140-5p/Aurora-a signaling in hepatocellular carcinoma. *Molecular Cancer Therapeutics*, *19*, 1197–1209.
- Gao, L. Y., Hao, X. L., Zhang, L., Wan, T., Liu, J. Y., & Cao, J. (2020). Identification and characterization of differentially expressed lncRNA in 2,3,7,8-tetrachlorodibenzo-p-dioxin-induced cleft palate. *Human & Experimental Toxicology*, *39*, 748–761.
- Gao, L., Liu, Y., Wen, Y., & Wu, W. (2017a). LncRNA H19-mediated mouse cleft palate induced by all-trans retinoic acid. *Human & Experimental Toxicology*, *36*, 395–401. <https://doi.org/10.1177/0960327116651121>
- Gao, L. Y., Zhang, F. Q., Zhao, W. H., Han, G. L., Wang, X., Li, Q., Gao, S. S., & Wu, W. D. (2017b). LncRNA H19 and target gene-mediated cleft palate induced by TCDD. *Biomedical and Environmental Sciences : BES*, *30*, 676–680.
- Garber, M., Grabherr, M. G., Guttman, M., & Trapnell, C. (2011). Computational methods for transcriptome annotation and quantification using RNA-seq. *Nature Methods*, *8*, 469–477.
- Halbritter, J., Bizet, A. A., Schmidts, M., Porath, J. D., Braun, D. A., Gee, H. Y., McInerney-Leo, A. M., Krug, P., Filhol, E., Davis, E. E., Airik, R., Czarnecki, P. G., Lehman, A. M., Trnka, P., Nitschké, P., Bole-Feysoy, C., Schueler, M., Knebelmann, B., Burtey, S., ... Hildebrandt, F. (2013). Defects in the IFT-B component IFT172 cause Jeune and Mainzer-Saldino syndromes in humans. *American Journal of Human Genetics*, *93*, 915–925.
- Hall, M. D., Murray, C. A., Valdez, M. J., & Perantoni, A. O. (2017). Mesoderm-specific Stat3 deletion affects expression of Sox9 yielding Sox9-dependent phenotypes. *PLoS Genetics*, *13*, e1006610.
- Hammond, N. L., Dixon, J., & Dixon, M. J. (2019). Periderm: Life-cycle and function during orofacial and epidermal development. *Seminars in Cell & Developmental Biology*, *91*, 75–83.
- Hong, J., Guo, F., Lu, S.-Y., Shen, C., Ma, D., Zhang, X., Xie, Y., Yan, T., Yu, T., Sun, T., Qian, Y., Zhong, M., Chen, J., Peng, Y., Wang, C., Zhou, X., Liu, J., Liu, Q., Ma, X., ... Fang, J.-Y. (2020a). *F. nucleatum* targets lncRNA ENO1-IT1 to promote glycolysis and oncogenesis in colorectal cancer. *Gut*, *70*(11), 2123–2137.
- Hong, S., Hu, S., Kang, Z., Liu, Z., Yang, W., Zhang, Y., Yang, D., Ruan, W., Yu, G., Sun, L., & Chen, L. (2020b). Identification of functional lncRNAs based on competing endogenous RNA network in osteoblast differentiation. *Journal of Cellular Physiology*, *235*, 2232–2244. <https://doi.org/10.1002/jcp.29132>
- Ilott, N. E., Heward, J. A., Roux, B., Tsiouli, E., Fenwick, P. S., Lenzi, L., Goodhead, I., Hertz-Fowler, C., Heger, A., Hall, N., Donnelly, L. E., Sims, D., & Lindsay, M. A. (2014). Long non-coding RNAs and enhancer RNAs regulate the lipopolysaccharide-induced inflammatory response in human monocytes. *Nature Communications*, *5*, 3979.
- Jarroux, J., Morillon, A., & Pinskaya, M. (2017). History, discovery, and classification of lncRNAs. *Advances in Experimental Medicine and Biology*, *1008*, 1–46.
- Jia, S., Zhou, J., Fanelli, C., Wee, Y., Bonds, J., Schneider, P., Mues, G., & D'Souza, R. N. (2017). Small-molecule Wnt agonists correct cleft palates in Pax9 mutant mice in utero. *Development*, *144*, 3819–3828.
- Jin, C., Zheng, Y., Huang, Y., Liu, Y., Jia, L., & Zhou, Y. (2017). Long non-coding RNA MIAT knockdown promotes osteogenic differentiation of human adipose-derived stem cells. *Cell Biology International*, *41*, 33–41.
- Kanehisa, M., & Goto, S. (2000). KEGG: Kyoto encyclopedia of genes and genomes. *Nucleic Acids Research*, *28*, 27–30.
- Kim, D., Paggi, J. M., Park, C., Bennett, C., & Salzberg, S. L. (2019). Graph-based genome alignment and genotyping with HISAT2 and HISAT-genotype. *Nature Biotechnology*, *37*, 907–915.
- Langfelder, P., & Horvath, S. (2008). WGCNA: An R package for weighted correlation network analysis. *BMC Bioinformatics*, *9*, 559.
- Leng, N., Dawson, J. A., Thomson, J. A., Ruotti, V., Rissman, A. I., Smits, B. M. G., Haag, J. D., Gould, M. N., Stewart, R. M., & Kendziorski, C. (2013). EBSeq: an empirical Bayes hierarchical model for inference in RNA-seq experiments. *Bioinformatics (Oxford, England)*, *29*, 1035–1043.
- Li, A., Mallik, S., Luo, H., Jia, P., Lee, D. F., & Zhao, Z. (2020). H19, a long non-coding RNA, mediates transcription factors and target genes through interference of microRNAs in Pan-Cancer. *Molecular Therapy. Nucleic Acids*, *21*, 180–191.
- Li, C., Lan, Y., & Jiang, R. (2017). Molecular and cellular mechanisms of palate development. *Journal of Dental Research*, *96*, 1184–1191.
- Li, H., Yu, B., Li, J., Su, L., Yan, M., Zhang, J., Li, C., Zhu, Z., & Liu, B. (2015). Characterization of differentially expressed genes involved in pathways associated with gastric cancer. *PLoS One*, *10*, e0125013.
- Li, J., Rodriguez, G., Han, X., Janečková, E., Kahng, S., Song, B., & Chai, Y. (2019). Regulatory mechanisms of soft palate development and malformations. *Journal of Dental Research*, *98*, 959–967.
- Li, L., Shi, J. Y., Zhu, G. Q., & Shi, B. (2012). MiR-17-92 cluster regulates cell proliferation and collagen synthesis by targeting TGFβ pathway in mouse palatal mesenchymal cells. *Journal of Cellular Biochemistry*, *113*, 1235–1244.
- Liu, X., Zhang, Y., Shen, L., He, Z., Chen, Y., Li, N., Zhang, X., Zhang, T., Gao, S., Yue, H., Li, Z., & Yu, Z. (2021). LncRNA Meg3-mediated regulation of the Smad pathway in atRA-induced cleft palate. *Toxicology Letters*, *341*, 51–58.
- Lough, K. J., Byrd, K. M., Spitzer, D. C., & Williams, S. E. (2017). Closing the Gap: Mouse models to study adhesion in secondary palatogenesis. *Journal of Dental Research*, *96*, 1210–1220.
- Maimets, M., Pedersen, M. T., Guiu, J., Dreier, J., Thodberg, M., Antoku, Y., Schweiger, P. J., Rib, L., Bressan, R. B., Miao, Y., Garcia, K. C., Sandelin, A., Serup, P., & Jensen, K. B. (2022). Mesenchymal-epithelial crosstalk shapes intestinal regionalisation via Wnt and Shh signalling. *Nature Communications*, *13*, 715.
- Martinelli, M., Palmieri, A., Carinci, F., & Scapoli, L. (2020). Non-syndromic cleft palate: An overview on human genetic and environmental risk factors. *Frontiers in Cell and Developmental Biology*, *8*, 592271.
- Mukhopadhyay, P., Brock, G., Pihur, V., Webb, C., Pisano, M. M., & Greene, R. M. (2010). Developmental microRNA expression profiling of murine embryonic orofacial tissue. *Birth Defects Research. Part A, Clinical and Molecular Teratology*, *88*, 511–534.
- Nandadasa, S., Kraft, C. M., Wang, L. W., O'Donnell, A., Patel, R., Gee, H. Y., Grobe, K., Cox, T. C., Hildebrandt, F., & Apte, S. S. (2019). Secreted metalloproteases ADAMTS9 and ADAMTS20 have a non-canonical role in ciliary vesicle growth during ciliogenesis. *Nature Communications*, *10*, 953.
- Ning, G., Liu, X., Dai, M., Meng, A., & Wang, Q. (2013). MicroRNA-92a upholds Bmp signaling by targeting noggin3 during pharyngeal cartilage formation. *Developmental Cell*, *24*, 283–295.
- Ozturk, F., Li, Y., Zhu, X., Guda, C., & Nawshad, A. (2013). Systematic analysis of palatal transcriptome to identify cleft palate genes within TGFβ3-knockout mice alleles: RNA-Seq analysis of TGFβ3 mice. *BMC Genomics*, *14*, 113.
- Parker, S. E., Mai, C. T., Canfield, M. A., Rickard, R., Wang, Y., Meyer, R. E., Anderson, P., Mason, C. A., Collins, J. S., Kirby, R. S., & Correa, A. (2010). Updated national birth prevalence estimates for selected birth defects in the United States, 2004–2006. *Birth Defects Research. Part A, Clinical and Molecular Teratology*, *88*, 1008–1016.
- Peng, Y., Wang, X. H., Su, C. N., Qiao, W. W., Gao, Q., Sun, X. F., & Meng, L. Y. (2020). RNA-seq analysis of palatal transcriptome changes in all-trans retinoic acid-induced cleft palate of mice. *Environmental Toxicology and Pharmacology*, *80*, 103438.
- Priest, A. V., Shafraz, O., & Sivasankar, S. (2017). Biophysical basis of cadherin mediated cell-cell adhesion. *Experimental Cell Research*, *358*, 10–13.

- Rehmsmeier, M., Steffen, P., Hochsmann, M., & Giegerich, R. (2004). Fast and effective prediction of microRNA/target duplexes. *RNA (New York, N.Y.)*, *10*, 1507–1517.
- Richardson, R. J., Hammond, N. L., Coulombe, P. A., Saloranta, C., Nousiainen, H. O., Salonen, R., Berry, A., Hanley, N., Headon, D., Karikoski, R., & Dixon, M. J. (2014). Periderm prevents pathological epithelial adhesions during embryogenesis. *J Clin Invest*, *124*, 3891–3900.
- Ritter, N., Ali, T., Kopitchinski, N., Schuster, P., Beisaw, A., Hendrix, D. A., Schulz, M. H., Müller-McNicol, M., Dimmeler, S., & Grote, P. (2019). The lncRNA locus handsdown regulates cardiac gene programs and is essential for early mouse development. *Developmental Cell*, *50*, 644–657.e8.
- Sarkar, L., Cobourne, M., Naylor, S., Smalley, M., Dale, T., & Sharpe, P. T. (2000). Wnt/Shh interactions regulate ectodermal boundary formation during mammalian tooth development. *Proceedings of the National Academy of Sciences*, *97*, 4520–4524.
- Schoen, C., Aschrafi, A., Thonissen, M., Poelmans, G., Von den Hoff, J. W., & Carels, C. E. L. (2017). MicroRNAs in palatogenesis and cleft palate. *Frontiers in Physiology*, *8*, 165.
- Shin, J. O., Lee, J. M., Cho, K. W., Kwak, S., Kwon, H. J., Lee, M. J., Cho, S. W., Kim, K. S., & Jung, H. S. (2012a). MiR-200b is involved in Tgf- β signaling to regulate mammalian palate development. *Histochemistry and Cell Biology*, *137*, 67–78. <https://doi.org/10.1007/s00418-011-0876-1>
- Shin, J. O., Nakagawa, E., Kim, E. J., Cho, K. W., Lee, J. M., Cho, S. W., & Jung, H. S. (2012b). miR-200b regulates cell migration via Zeb family during mouse palate development. *Histochemistry and Cell Biology*, *137*, 459–470. <https://doi.org/10.1007/s00418-012-0915-6>
- Shu, X., Dong, Z., & Shu, S. (2019a). AMBRA1-mediated autophagy and apoptosis associated with an epithelial-mesenchymal transition in the development of cleft palate induced by all-trans retinoic acid. *Annals of Translational Medicine*, *7*, 128. <https://doi.org/10.21037/atm.2019.02.22>
- Shu, X., Dong, Z., Zhang, M., & Shu, S. (2019b). Integrated analysis identifying long non-coding RNAs (lncRNAs) for competing endogenous RNAs (ceRNAs) network-regulated palatal shelf fusion in the development of mouse cleft palate. *Annals of Translational Medicine*, *7*, 762. <https://doi.org/10.21037/atm.2019.11.93>
- Shu, X., Shu, S., & Cheng, H. (2019c). A novel lncRNA-mediated trans-regulatory mechanism in the development of cleft palate in mouse. *Molecular Genetics & Genomic Medicine*, *7*, e00522.
- Statello, L., Guo, C. J., Chen, L. L., & Huarte, M. (2021). Gene regulation by long non-coding RNAs and its biological functions. *Nature Reviews Molecular Cell Biology*, *22*, 96–118.
- Sulik, K., Dehart, D. B., Ilangaki, T., Carson, J. L., Vrablic, T., Gesteland, K., & Schoenwolf, G. C. (1994). Morphogenesis of the murine node and notochordal plate. *Developmental Dynamics: An Official Publication of the American Association of Anatomists*, *201*, 260–278.
- Thauvin-Robinet, C., Lee, J. S., Lopez, E., Herranz-Pérez, V., Shida, T., Franco, B., Jego, L., Ye, F., Pasquier, L., Loget, P., Gigot, N., Aral, B., Lopes, C. A., St-Onge, J., Bruel, A. L., Thevenon, J., González-Granero, S., Alby, C., Munnich, A., ... Nachury, M. V. (2014). The oral-facial-digital syndrome gene C2CD3 encodes a positive regulator of centriole elongation. *Nature Genetics*, *46*, 905–911.
- Uziel, T., Karginov, F. V., Xie, S., Parker, J. S., Wang, Y. D., Gajjar, A., He, L., Ellison, D., Gilbertson, R. J., Hannon, G., & Rousset, M. F. (2009). The miR-17-92 cluster collaborates with the Sonic Hedgehog pathway in medulloblastoma. *Proceedings of the National Academy of Sciences of the United States of America*, *106*, 2812–2817.
- Vogelaar, I. P., Figueiredo, J., van Rooij, I. A., Simões-Correia, J., van der Post, R. S., Melo, S., Seruca, R., Carels, C. E., Ligtenberg, M. J., & Hoogerbrugge, N. (2013). Identification of germline mutations in the cancer predisposing gene CDH1 in patients with orofacial clefts. *Human Molecular Genetics*, *22*, 919–926.
- Wang, F., Ren, D., Liang, X., Ke, S., Zhang, B., Hu, B., Song, X., & Wang, X. (2019). A long noncoding RNA cluster-based genomic locus maintains proper development and visual function. *Nucleic Acids Research*, *47*, 6315–6329.
- Wang, J., Bai, Y., Li, H., Greene, S. B., Klysik, E., Yu, W., Schwartz, R. J., Williams, T. J., & Martin, J. F. (2013). MicroRNA-17-92, a direct Ap-2 α transcriptional target, modulates T-box factor activity in orofacial clefting. *PLoS Genetics*, *9*, e1003785.
- Wang, Z., Gerstein, M., & Snyder, M. (2009). RNA-Seq: A revolutionary tool for transcriptomics. *Nature Reviews. Genetics*, *10*, 57–63.
- Waters, A. M., & Beales, P. L. (2011). Ciliopathies: An expanding disease spectrum. *Pediatric Nephrology (Berlin, Germany)*, *26*, 1039–1056.
- Yeung, K. S., Chee, Y. Y., Luk, H. M., Kan, A. S., Tang, M. H., Lau, E. T., Shuen, A. Y., Lo, I. F., Chan, K. Y., & Chung, B. H. (2014). Spread of X inactivation on chromosome 15 is associated with a more severe phenotype in a girl with an unbalanced t(X; 15) translocation. *American Journal of Medical Genetics. Part A*, *164a*, 2521–2528.
- Yuan, G., Singh, G., Chen, S., Perez, K. C., Wu, Y., Liu, B., & Helms, J. A. (2017). Cleft palate and aglossia result from perturbations in Wnt and hedgehog signaling. *Cleft Palate-Craniofacial Journal*, *54*, 269–280.
- Yun, L., Ma, L., Wang, M., Yang, F., Kan, S., Zhang, C., Xu, M., Li, D., Du, Y., Zhang, W., Pan, Y., & Wang, L. (2019). Rs2262251 in lncRNA RP11-462G12.2 is associated with nonsyndromic cleft lip with/without cleft palate. *Human Mutation*, *40*, 2057–2067.
- Zhong, W., Zhao, H., Huang, W., Zhang, M., Zhang, Q., Zhang, Y., Chen, C., Nueraihemaiti, Z., Tuerhong, D., Huang, H., Maimaitili, G., Chen, F., & Lin, J. (2021). Identification of rare PTCH1 nonsense variant causing orofacial cleft in a Chinese family and an up-to-date genotype-phenotype analysis. *Genes & Diseases*, *8*(5), 689–697. <https://doi.org/10.1016/j.gendis.2019.12.010>
- Zhou, M., Ma, J., Chen, S., Chen, X., & Yu, X. (2014). MicroRNA-17-92 cluster regulates osteoblast proliferation and differentiation. *Endocrine*, *45*, 302–310.

SUPPORTING INFORMATION

Additional supporting information may be found in the online version of the article at the publisher's website.

How to cite this article: Huang, W., Zhong, W., He, Q., Xu, Y., Lin, J., Ding, Y., Zhao, H., Zheng, X., & Zheng, Y. (2023). Time-series expression profiles of mRNAs and lncRNAs during mammalian palatogenesis. *Oral Diseases*, *29*, 2163–2176. <https://doi.org/10.1111/odi.14237>